THE ATLANTIC MULTIDECADAL OSCILLATION: A CLARIFICATION AND CHARACTERIZATION AT DEPTHS

Benjamin T. Moffat[1] and Michael J. Schirripa[2]

SUMMARY

The objective of this study was to investigate the projected Atlantic Multidecadal Oscillation (AMO) at depths inhabited by highly migratory species. This is possible using volumetric temperature data projected to 2050 at several depths (GFDL-ESM4.1). When recreating the sea surface AMO index with the ESM4.1 dataset, we discovered that the signal did not align with others previously published. It became evident that the AMO is expressed differently, in some cases producing conflicting warm-cool phases, depending on the data source, the time scale upon which it is averaged, and the detrending methodology. The strengths and weaknesses of the two types of available data (simulation-based and observation-based) and existing detrending methods are discussed. Using ESM4.1, we characterized the AMO signal at depths. Signals were analyzed for regime shifts of statistically significant warm and cool phases. Notable results include compression of the signal with depth and delayed regime shifts with depth. Signals at a peak warm and cool phase year were mapped at several depths for a spatial temperature comparison illustrating a greater temperature discrepancy at lower latitudes and towards the sea surface.

KEYWORDS

Habitat, Environmental Effects, Surface Temperature

[1] Rosenstiel School of Marine and Atmospheric Science, 4600 Rickenbacker Causeway, Miami, FL 33149 USA, btm76@miami.edu
[2] NOAA Fisheries, Southeast Fisheries Science Center, 75 Virginia Beach Drive, Miami, FL, 33149 USA. Michael.schirripa@noaa.gov

Introduction

The Atlantic Multidecadal Oscillation (AMO) is an observed oceanographic phenomenon referring to large-scale low-frequency variability in the Atlantic Ocean. The AMO index indicates warm and cool phases of averaged anomalies of sea surface temperature (SST) variability in the North Atlantic Ocean. The index has an estimated period of 60 to 80 years and an amplitude of 0.2 to 0.5º C. It is often detrended from the linear climate change signal by subtracting the global-mean SST from the spatially averaged time series of the AMO (Trenberth and Shea 2006). To be more precise, the AMO is calculated by taking the annual average of temperature values from each 1º by 1º grid point, typically from 0º - 80º N, 55º W - 5º E, and subtracting it from the total average over all years (Enfield et al. 2001). Studies have demonstrated the AMO influence on atmospheric and environmental variability, including shifts in hurricane activity, rainfall patterns, and the distribution of marine organisms (Trenberth and Shea 2006, Enfield et al. 2001, Edwards et al. 2013).

Previous studies that investigated the relationship between the AMO and North Atlantic fisheries have suggested several possible interactions. In one study, researchers used area-specific catch rates of North Atlantic Swordfish to detect basin-wide responses to changing oceanography. They found when the AMO was in a warm phase, the CPUE in the west Atlantic basin was higher and the east was lower, possibly due to shifts in preferred habitat or prey species (Schirripa et al. 2017). Other studies found similar coinciding events with temperature increases and swordfish abundance in the North Atlantic pertaining to the AMO (Mejuto et al. 2017, Sunby et al. 2013). Researchers studying Atlantic bluefin tuna demonstrated a prevailing influence of the AMO on both their abundance and distribution, as well as the role of the AMO in both the collapse and revival of the highly valued stock during a cool and warm phase, respectively (Faillettaz et al., 2019). One shared conclusion among these studies is that climatic variability should be incorporated in stock management plans as environmental conditions strongly and predictably influence population dynamics.

Highly migratory species (HMS) of fish in the North Atlantic Ocean, including species of tuna, swordfish, billfish, and shark, spend much of their time in the mid-water column, sometimes diving as deep as 900 meters (Goodyear et al. 2006). One analysis of the AMO imprint at varying depths exists, and the study was limited to 400m and a short time scale (Frankcombe et al. 2008). Each species has its temperature preference and behavior regarding regulating body temperature. Logically, knowledge of thermal variability in the ocean is crucial to understanding these fish's migration and movement. Therefore, analysis of the imprint of the AMO at depths and over long periods would be useful to a species distribution model to improve understanding of the population dynamics and better inform fisheries management. Furthermore, a projection of the AMO into the future can enhance Atlantic HMS management to an even greater extent by forecasting the spatial distribution of these fisheries.

1. A Clarification of the AMO

The AMO's characterization depends on the temperature dataset used, the time scale upon which it is averaged, and the methods used, if any, to detrend the index from the averaged global ocean temperature trend. This adds a great deal of input variability, begging the question – what is the *real* AMO? A standardized or widely agreed-upon methodology for the index does not currently exist for any of the factors mentioned (data, timescale, or detrending methods). This is evident in the literature as several published papers refer to AMO indices that are not consistent with one another (Frajka-Williams et al., 2017, Frankignoul et al., 2017, Faillettaz 2019). From a fisheries perspective, this is concerning due to the potential for poor management actions inferred from inconsistent indices between studies.

Two types of data are commonly used to characterize the AMO, simulation-based and observation-based. The AMO has a significant component due to natural variability meaning that it is influenced by a complex combination of many dynamic factors, some understood and some unknown. The simulated datasets are created from varying external forcing models that are expected to have considerably different natural variability and therefore expression, as seen in **Figure 1**. These datasets vary substantially in representing the forced component due to differences in their prescribed external forcing (CO_2, volcanoes, methane, etc.). It is challenging to separate forcing from both greenhouse gasses and aerosols, which cool the ocean, from the internal variability in the system. Therefore, the simulation-based datasets contain considerable uncertainty with the complex nature of internal variability and errors in the force response, limiting the predictability power and robustness of the data.

Observational estimates for oceanographic temperature data (such as HadISST) are based on in situ observations and are subsequently gridded. However, they also hold uncertainty (although less so than simulated data) mainly due to gaps in data coverage and the methods utilized for gridding or interpolation. The strengths and weaknesses

of the various SST observations are discussed in the NCAR climate data guide, along with pointers to the various observational estimates (National Center for Atmospheric Research, 2014). Therefore, the best practice is to use observational-based data for historical studies and simulated-based data to project possible future conditions. For the longest historical records, COBE data or the HadISST data are a common choice.

The timescale upon which the AMO is averaged affects the expression of the signal as well. Since the AMO is essentially the detrended sea temperature anomaly, the mean value on which the anomaly is calculated has a significant effect on its expression. For instance, one can imagine the different expressions from a study looking at 1900 – 2000 versus 1950 – 2000 as the averaged ocean temperature would differ based on the extent of warm and cool phases in the respective period. Accordingly, researchers should be cautious of the mean value used when creating the AMO in different timeframes and make any necessary adjustments.

Lastly, there are several detrending methods that exist to remove the global forced trend from the AMO index which affects the expression of the multidecadal signal (Deser and Phillips, 2021). The most common include subtracting the mean temperature of the entirety of the global ocean or subtracting the mean temperature of the global ocean temperature outside of the intended study area from the index (the average ocean temperature outside the North Atlantic for the AMO, Trenberth and Shea 2006, Enfield et al. 2001). Different AMO signals will be expressed depending on how this external temperature forcing is removed, including when the zero-crossing occurs (when the warm-cool phase transitions occur). If using an ensemble of simulations (many runs with the same model and greenhouse gas forcing), the best way to remove the forced trend is to subtract the ensemble mean from each simulation. Several alternative options exist if a single simulation or a small subset of runs is used and there is a need to remove the forced signal.

Additionally, data challenges exist for sea temperature at depth simply because much fewer subsurface data exist than at the surface, prior to the Argo era. Starting in 2004, the international Argo program measures water properties across the world's ocean using a fleet of robotic instruments that drift with the ocean currents and move up and down between the surface and a mid-water level. Other methods to obtain sea temperature at depth include using an ocean reanalysis, which combines observations with a model to produce 3-D gridded fields. There are several ocean reanalyses. One with a longer record is the Simple Ocean Data Assimilation (SODA) reanalysis and other versions go back to 1958. There are also ocean products that use statistical methods to obtain gridded values.

It is worth noting that from observational estimates, the fluctuations occur over a long time. Hence, it's not clear if there is an actual oscillatory period or if it has variability at long time scales with no preferred period, also known as a red noise process. This remains a topic of scientific debate.

Until there is a consensus on a standard for the index, we would like to emphasize the importance of clearly stating the data source, timescale used for averaging, and detrending methods when presenting any conclusions based on produced AMO signals.

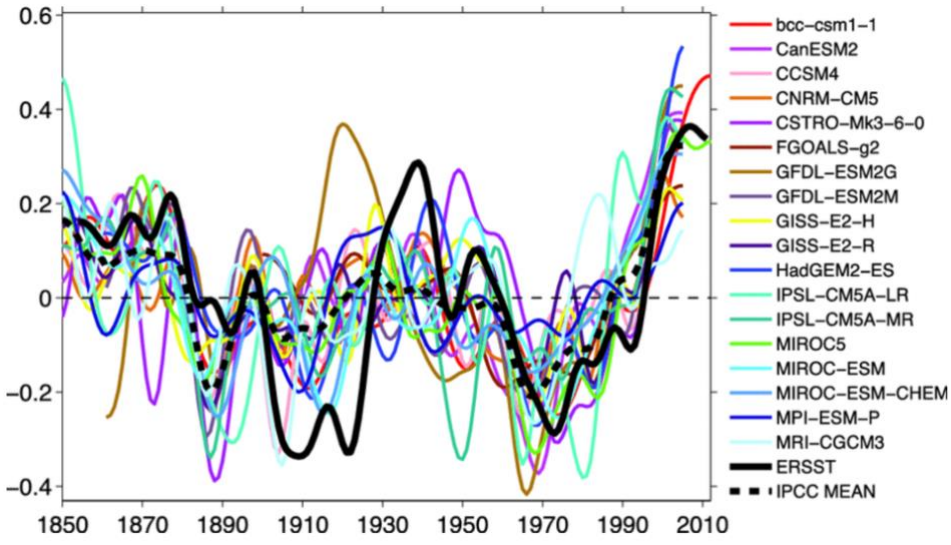

Figure 1. Observed and simulated AMO index from several models, and the observational estimates

2. Data and Methods

2.1 Data Source and Assumptions

This study used volumetric temperature data from the NOAA Geophysical Fluid Dynamics Laboratory Earth System Model version 4.1 (GFDL-ESM4.1), which includes simulated temperatures from 1900 to 2050 at 46 depth layers ranging from 0 to 1968 meters deep. The ESM4.1 simulation tools are based on an atmospheric circulation model coupled with an oceanic circulation model representing land, sea ice, and iceberg dynamics. ESMs incorporate interactive biogeochemistry, including the carbon cycle. The oceanic component includes features such as free surface to capture wave processes; water fluxes or flow; currents; sea ice dynamics; iceberg transport of freshwater; and a state-of-the-art representation of ocean mixing and marine biogeochemistry and ecology.

2.2 AMO Calculation

We use a time period of 1960 to 2050 for the projected AMO index and characterize the signal at each of the 46 depth layers available. We chose these years for the time frame for two reasons. First, most models are in alignment from 1960 onward, as seen in **Figure 1**. Second, this time frame encompasses a full cool and warm phase. Cleaning and manipulation of the data set were performed in R using the *dplyr* package. The data was filtered to years of interest and to all latitudes greater than zero (as the highest latitude in the ESM4.1 data is 65.5 degrees). We averaged the annual temperatures across the North Atlantic basin and subtracted them from the mean temperature of 1960 to 2050 at each depth layer respectively. The oscillation was detrended by subtracting the averaged temperature trend from the remainder of the dataset (the non-filtered data), outside of the North Atlantic.

2.3 Regime Shift Detection

Regime shifts are defined as rapid reorganizations of ecosystems from one relatively stable state to another. In the marine environment, regimes may last for several decades, and shifts often appear to be associated with changes in the climate system, as is the case for the AMO. There are several methods designed to detect regime shifts in both the individual time series and entire systems (Rodionov 2004). However, most of these methods experience deterioration in their performance toward the end of the time series. Rodionov (2005a) developed a new approach based on a sequential t-test that can signal a possibility of a regime shift in real-time. The code for the method is written in Visual Basic for Application (Excel). The program can detect shifts in both the mean level of fluctuations and the variance. The algorithm for the variance is like that for the mean but based on a sequential F-test (Rodionov 2005b).

Using a sequential data processing technique, the number of observations is not fixed but comes in sequence. For each new observation, a test is performed to determine the validity of the null hypothesis, H0 (the existence of a regime shift). There are three possible outcomes of the test: accept H0, reject H0, or keep testing.

First, the cut-off length (l) of the regimes is set to be determined for variable X. The parameter l is akin to the cut-off point in low-pass filtering. Essentially, the length of each expected regime shift. Second, the difference *diff* between the mean values of two subsequent regimes is determined that would be statistically significant according to the Student's t-test:

$$diff = t\sqrt{2\sigma_l^2/l},$$

Where t is the value of t-distribution with $2l - 2$ degrees of freedom at the given probability level p. It is assumed that the variances for both regimes are the same and equal to the average variance for running l-year intervals in the time series of variable X. Third, the mean of the initial l values of variable X is calculated as an estimate for regime $R1$, and the levels that should be reached in the subsequent l years to qualify for a shift to regime $R2$. Next, each new value starting with the year $I = l + 1$ is checked for whether it is greater than the mean $R1 + diff$ or less than the mean $R1 - diff$. If it does not exceed the mean $R1 \pm diff$ range, it is assumed that the current regime has not changed. In this case, recalculate the average mean $R1$ to include the new and previous values of variable X and wait for the following value. If the new value exceeds the mean $R1 \pm diff$ range, then this year is considered as a possible start point j of the new regime $R2$. After the shift point is established, each new value where $I > j$ is used to confirm or reject the null hypothesis of a regime shift at year j. If the anomaly is of the same sign as the one at a regime shift, it will increase the confidence that the shift did occur. The reverse is true if the anomalies

have opposite signs. This change in the confidence of a regime shift at $I = j$ is reflected in the value of the regime shift index (RSI), which represents a cumulative sum of the normalized anomalies:

$$\mathrm{RSI}_{i,j} = \sum_{i=j}^{j+m} \frac{x_i^*}{l\sigma_l}, m = 0, 1, \ldots, l-1.$$

The negative value of RSI means that the test for a regime shift at year *j* failed, in which case a zero was assigned to RSI. The average value mean of *R*1 is recalculated to include the current value, and keep testing the following values starting with $I = j + 1$ for their exceedance of the range mean *R*1 + *diff* as before. The positive value of RSI implies that the regime shift at year *j* is significant at the probability level *p*. In this case, the actual mean value is calculated for the new regime *R2*. At this point, it becomes the base one, against which the test will continue further. The search for the next shift to regime R3 starts from the year $I = j + 1$. This step back is necessary to make sure that the timing of the next regime shift is determined correctly, even if the actual duration of regime *R*2 was less than l year. The calculations continue in a loop of the previous steps until all data for variable *X* are processed.

We used version 3.2 of Rodionov's regime shift detection program to account for autocorrelation (Rodionov 2006). It uses a prewhitening procedure to remove the red noise component from the time series before applying a regime shift detection method. It does not intend to reveal the nature of climate regimes; it is simply a way to see whether these regimes can be more than just a red noise process. Two critical elements of the procedure are subsampling and bias correction of the estimates.

We use this algorithm to investigate the extent to which statistically significant warm and cool phases occur at the different depth layers with the projected AMO data. The limitations in using this method are that the user decides the most appropriate input parameters for choosing the probability level, the cutoff length, and the Huber parameter. For this study, we use a probability level of 0.05, a cutoff length of 60 years, and a Huber parameter of 5. This combination produced logical RSIs and an amount of sensitivity that caught the identifiable cool and warm phases but not the more minor variations between them.

2.4 Mapping

We map the AMO to compare a peak warm phase year (2050) and a peak cool phase year (1965) according to the projected sea surface AMO signal. For both years, maps were also created at depths of interest, including at sea surface, 200m, and 800m deep. Maps were created in R as raster data using the *ggmap* and *ggspatial* packages.

3. Results and conclusions

The ESM4.1 projected annual SST in **Figure 2** shows a steep overall increase in average SST from a minimum of 21.05°C to a maximum of 22.49 °C and a total average of 21.83°C. Although the general trend is an increase, there is a lot of year-to-year variability present throughout the SST time series.

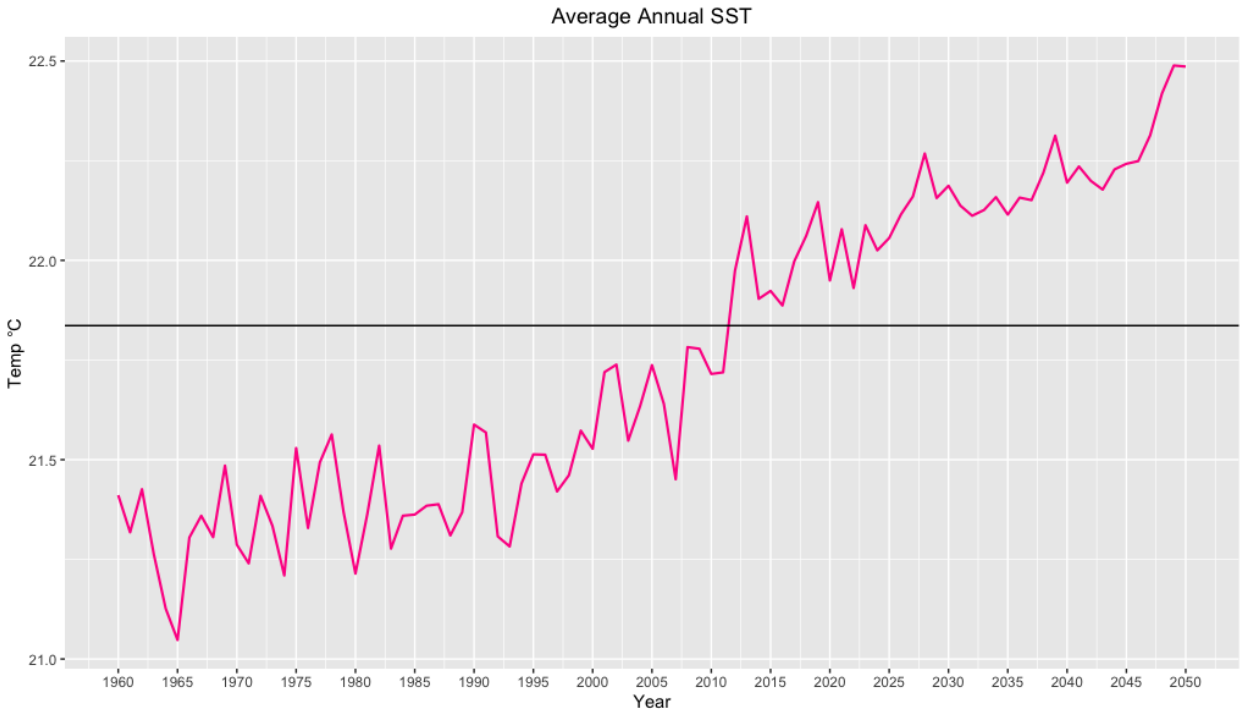

Figure 2. Averaged yearly temperatures in the North Atlantic Ocean from GFDL-ESM4.1. The horizontal line represents the average temperature from 1960 to 2050.

The AMO index was produced at nine depths using the previously explained methodology, as seen in **Figure 3**. The signal appears to compress with increasing depth, as indicated by the decreasing peak to trough temperature range. The minimum and maximum temperature differences between the 0-5m and the 878 – 984m depth layer are 1.44°C and 0.44°C, respectively. This is logical as there is more variation and factors affecting the sea surface (absorbed heat, wind, waves, ocean circulation) than the less mixed, cold, dense, deep water of the North Atlantic. Concerningly, in every depth layer, the warm phase continues to increase in temperature, not showing signs of flattening or decreasing by the end of the projected series in 2050. Although the cool phase to warm phase transition is easily seen in each AMO signal depth layer, the timing changes by a surprising margin.

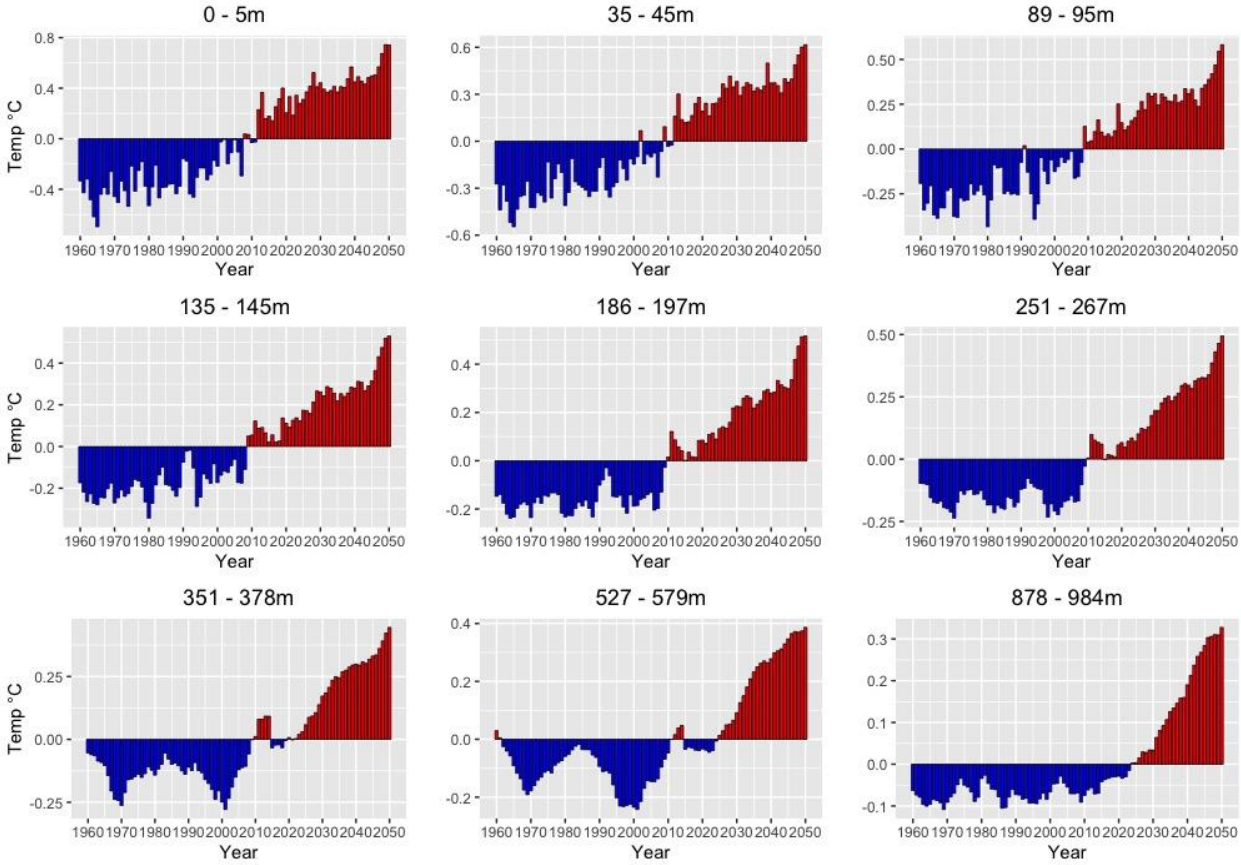

Figure 3. Projected AMO index for nine depth layers from 1960 to 2050. The y-axis scale does vary between plots.

Using the regime detection program described in the methods sections, a statistical measure was performed to quantify the timing and extent of differences between depths and the cool-warm phase transition. **Figure 4** shows the results from the regime shift detection. The input parameters were chosen to avoid the slight year-to-year variation and were used to indicate the statistically significant shift from the cool phase to the warm phase. Notably, the regime shift does not always occur where the projected average sea temperature crosses the zero line. It is evident that the AMO is not just a phenomenon at the sea surface but also has characteristics of periodic oscillations from a cool to warm phase at depths, even as deep as 984m (albeit with a smaller temperature flux).

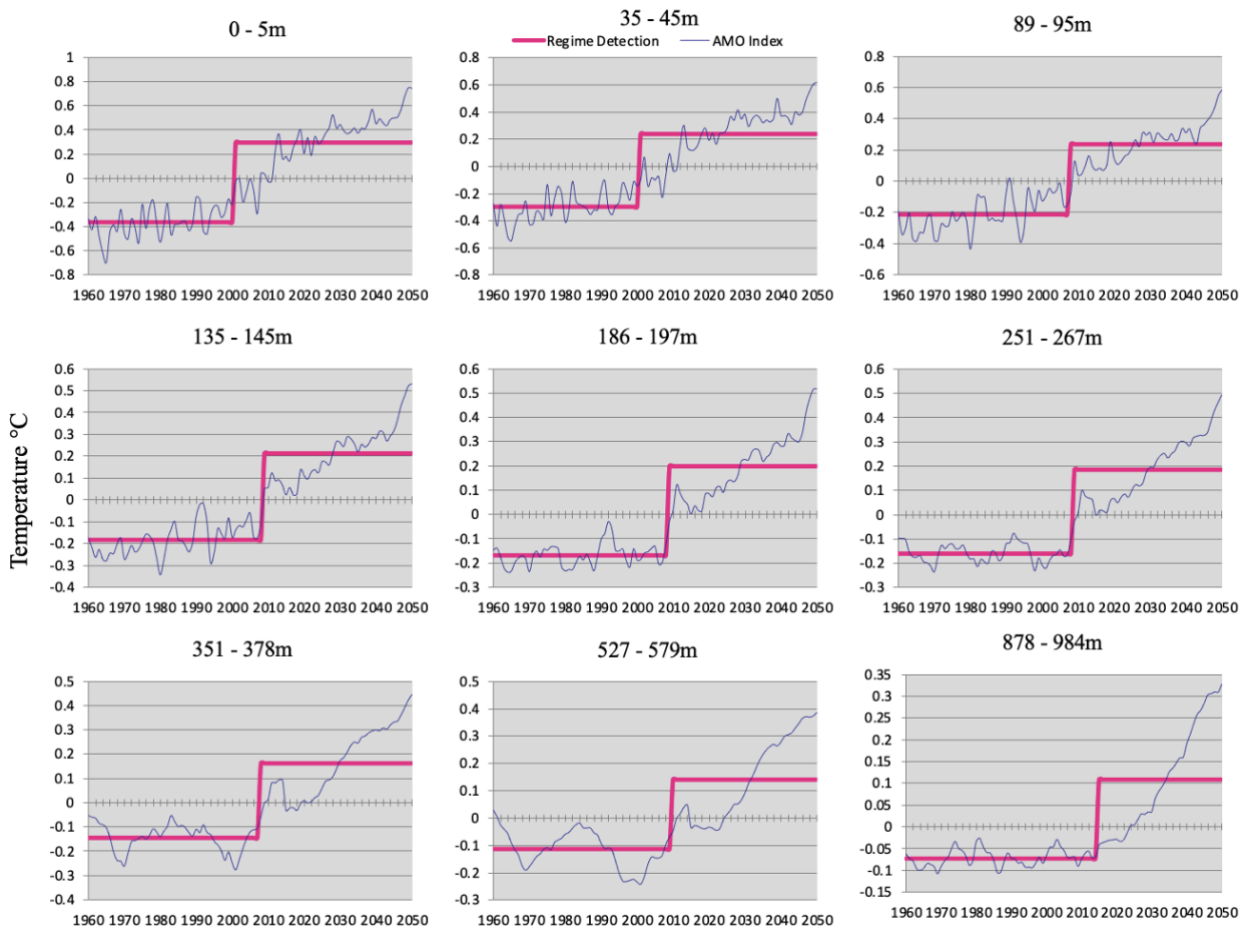

Figure 4. Regime shift detection analysis for each AMO signal at depth. Input parameters were l = 60, p = 0.05, and Huber parameter = 5 for all indices.

Figure 5 plots the timing of the shift against the depth of the AMO signal based on the values from the regime shift detection analysis (**Table 1**). Interestingly, the timing of the regime shift of the cool to warm phase from the AMO signal occurs later with increasing depth. The regime shift occurred in 2001 for the SST AMO index and 2015 for the AMO index at 878 – 984m deep. The regime shift index (RSI) for all regime shifts in each depth layer is extensive (>1), indicating a significant regime shift and a real cool to warm phase shift in each depth layer.

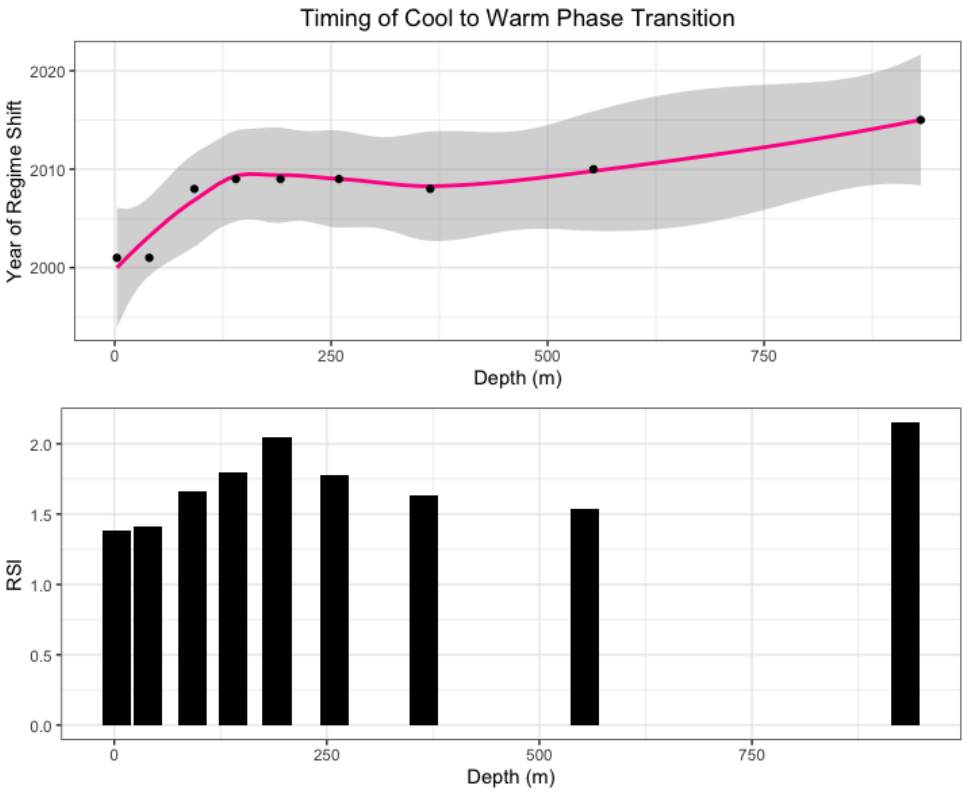

Figure 5. Top: Timing of regime shifts of the AMO cool to warm phase transitions at depth. Each point represents the depth layer analyzed, the pink line is the smoothed trend, and the shaded area is the 95% confidence interval. Bottom: Regime shift index and the extent of each cool to warm phase transition for each depth layer analyzed.

Table 1. Results from regime shift detection analysis using input parameters of $l = 60$, $p = 0.05$, and Huber parameter = 5.

Depth	Year of Shift	RSI
0 - 5m	2001	1.388
35 - 45m	2001	1.409
89 - 95m	2008	1.658
135 - 145m	2009	1.792
186 - 197m	2009	2.044
251 - 267m	2009	1.781
351 - 378m	2008	1.632
527 - 579m	2010	1.535
878 - 984m	2015	2.148

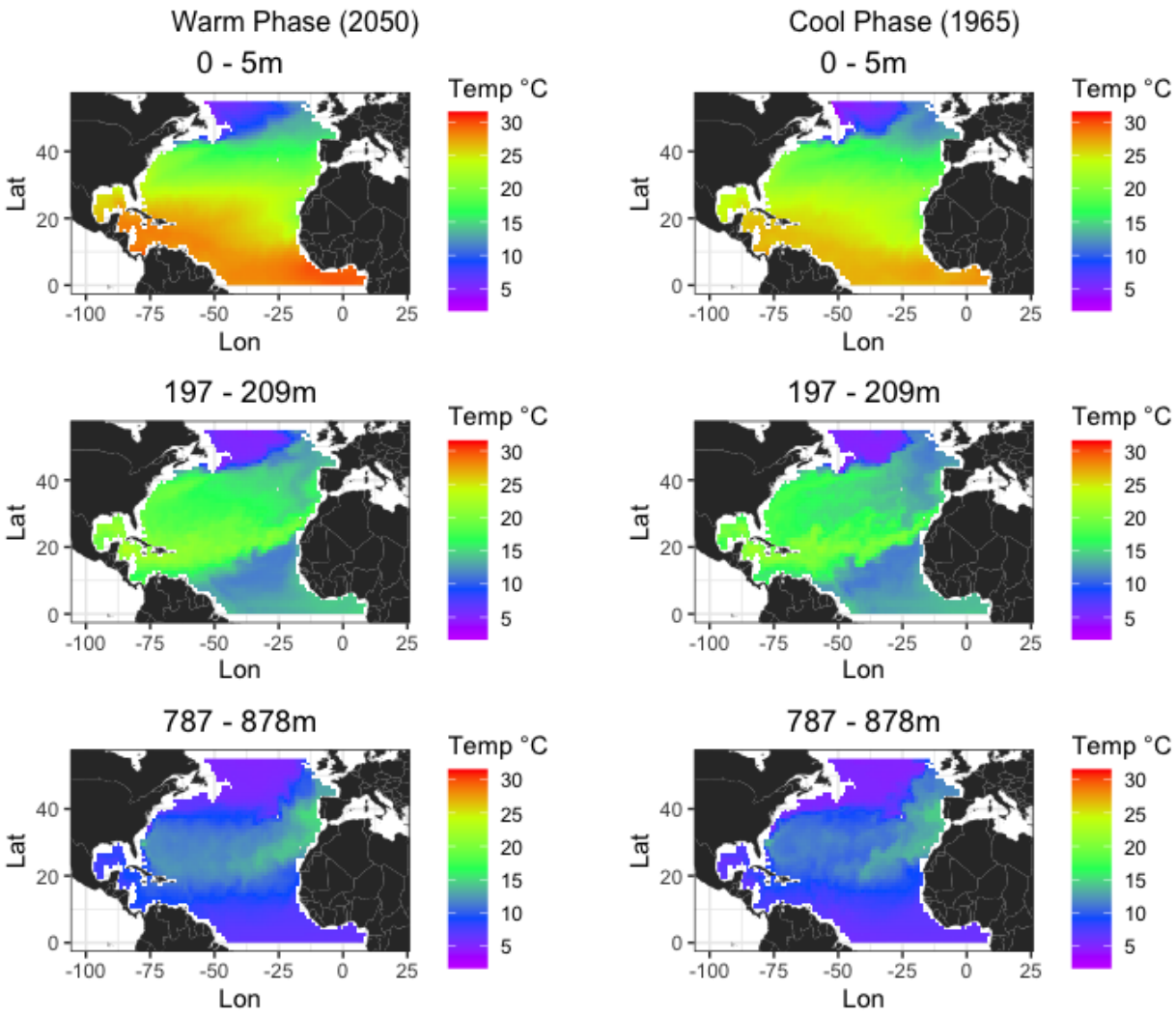

Figure 6. Maps of sea temperature at three depths: 0 – 5m (SST), 197 – 209m, and 787-878m. Maps in the left column are from the peak warm phase year of 2050. Maps in the right column are from the peak cool phase year of 1965.

The map comparison of a peak warm phase year versus a cool phase year in **Figure 6** agrees with the diminishing AMO signal with depth**.** An apparent discrepancy in temperature exists at the sea surface in which the warm phase year is much hotter towards the equator and in the Gulf of Mexico. However, from 20° latitude and northward, it looks similar to the cool year phase SST. At 197-209m deep, the warm phase year seems to show higher temperatures in the mid-north Atlantic than in the cool phase. At the deepest layer investigated, there are only very slight differences between the two years, as in agreeance with the AMO signal at this depth that showed an overall difference in average temperatures of 0.44°C.

This analysis of projected AMO signals at depth using the ESM4.1 dataset has demonstrated that the AMO signal exists at a statistically significant state beyond the sea surface. Furthermore, the signal is currently and continues to exist in an all-time high warm phase state, with projections showing increased averaged sea temperatures in the North Atlantic. We also found that the timing of the AMO regime shifts is delayed with increasing depth. The spatial differences of the AMO are more apparent in the lower latitudes and toward the sea surface. Standardization of the AMO calculation and guidelines for best practice (data source, time scale, detrending methods) would increase the consistency of signal characterization to the benefit of fisheries research and ultimately to the improvement of responsible HMS management.

4. Acknowledgments

Environmental data and **Figure 1** was provided by Natalie Perlin, Ph.D. and Ben Kirtman, Ph.D. I would also like to thank Ben Kirtman, Ph.D for his valuable insights and explanations of various AMO expression.

5. References

Deser, C. and A. S. Phillips, 2021: Defining the internal component of Atlantic Multidecadal Variability in a changing climate. Geophys. Res. Lett., 48, e2021GL095023, doi: 10.1029/2021GL095023.

Edwards, M., Beaugrand, G., Helaouët, P., Alheit, J., & Coombs, S. (2013). Marine ecosystem response to the Atlantic Multidecadal Oscillation. PloS one, 8(2), e57212.

Enfield, D. B., Mestas-Nuñez, A. M., & Trimble, P. J. (2001). The Atlantic multidecadal oscillation and its relation to rainfall and river flow in the continental US. Geophysical Research Letters, 28(10), 2077-2080.

Faillettaz, R., Beaugrand, G., Goberville, E., & Kirby, R. R. (2019). Atlantic Multidecadal Oscillations drive the basin-scale distribution of Atlantic bluefin tuna. *Science advances*, *5*(1).

Frajka-Williams, E., Beaulieu, C. & Duchez, A. (2017) Emerging negative Atlantic Multidecadal Oscillation index in spite of warm subtropics. Sci Rep 7, 11224. https://doi.org/10.1038/s41598-017-11046-x

Frankcombe, L. M., Dijkstra, H. A., & Von der Heydt, A. (2008). Sub-surface signatures of the Atlantic Multidecadal Oscillation. Geophysical Research Letters, 35(19).

Frankignoul, C., Gastineau, G., & Kwon, Y. O. (2017). Estimating the SST response to anthropogenic and external forcing and its impact on the Atlantic Multidecadal Oscillation and the Pacific Decadal Oscillation. Journal of Climate, 30(24), 9871–9895. https://doi.org/10.1175/jcli-d-17-0009.1

Goodyear, C. P., Luo, J., Prince, E. D., & Serafy, J. E. (2006). Temperature-depth habitat utilization of blue marlin monitored with PSAT tags in the context of simulation modeling of pelagic longline CPUE. Col. Vol. Sci. Pap. ICCAT, 59(1), 224-237.

Mejuto, J., García-Cortés, B., Ramos-Cartelle, A., & Fernández-Costa, J. (2017). Standardized catch rates in number of fish by age for the north Atlantic swordfish (Xiphias gladius) inferred from the Spanish longline fleet for the period 1982-2015 and environmental considerations. Collect. Vol. Sci. Pap. ICCAT, 74(3), 1208-1234.

National Center for Atmospheric Research Staff (Eds). Last modified 01 May 2014. "The Climate Data Guide: SST Data Sets: Overview & Comparison Table." Retrieved from https://climatedataguide.ucar.edu/climate-data/sst-data-sets-overview-comparison-table.

Nye, J. A., Baker, M. R., Bell, R., Kenny, A., Kilbourne, K. H., Friedland, K. D., ... & Wood, R. (2014). Ecosystem effects of the Atlantic multidecadal oscillation. Journal of Marine Systems, 133, 103-116.

Rodionov, S.N. (2004). A sequential algorithm for testing climate regime shifts. Geophys. Res. Lett., 31, L09204, doi:10.1029/2004GL019448.

Rodionov, S.N. (2005a). A brief overview of the regime shift detection methods. In: Large-Scale Disturbances (Regime Shifts) and Recovery in Aquatic Ecosystems: Challenges for Management Toward Sustainability, V. Velikova and N. Chipev (Eds.), UNESCO-ROSTE/BAS Workshop on Regime Shifts, 14-16 June 2005, Varna, Bulgaria, 17-24.

Rodionov, S.N. (2005b). Detecting regime shifts in the mean and variance: Methods and specific examples. In: Large-Scale Disturbances (Regime Shifts) and Recovery in Aquatic Ecosystems: Challenges for Management Toward Sustainability, V. Velikova and N. Chipev (Eds.), UNESCO-ROSTE/BAS Workshop on Regime Shifts, 14-16 June 2005, Varna, Bulgaria, 68-72.

Rodionov, S.N. (2006). The use of prewhitening in climate regime shift detection, Geophys. Res. Lett., 31, L12707, doi:101029/2006GL025904.

Schirripa, M. J., Abascal, F., Andrushchenko, I., Diaz, G., Mejuto, J., Ortiz, M., ... & Walter, J. (2017). A hypothesis of a redistribution of North Atlantic swordfish based on changing ocean conditions. Deep Sea Research Part II: Topical Studies in Oceanography, 140, 139-150.

Sundby, S., Nøttestad, L., Myklevoll, S., & Tangen, Ø. (2013). Swordfish towards the Arctic Atlantic in climate change. Collective Volume of Scientific Papers, 69, 1296-1303.

Trenberth, K. E., & Shea, D. J. (2006). Atlantic hurricanes and natural variability in 2005. Geophysical research letters, 33(12).